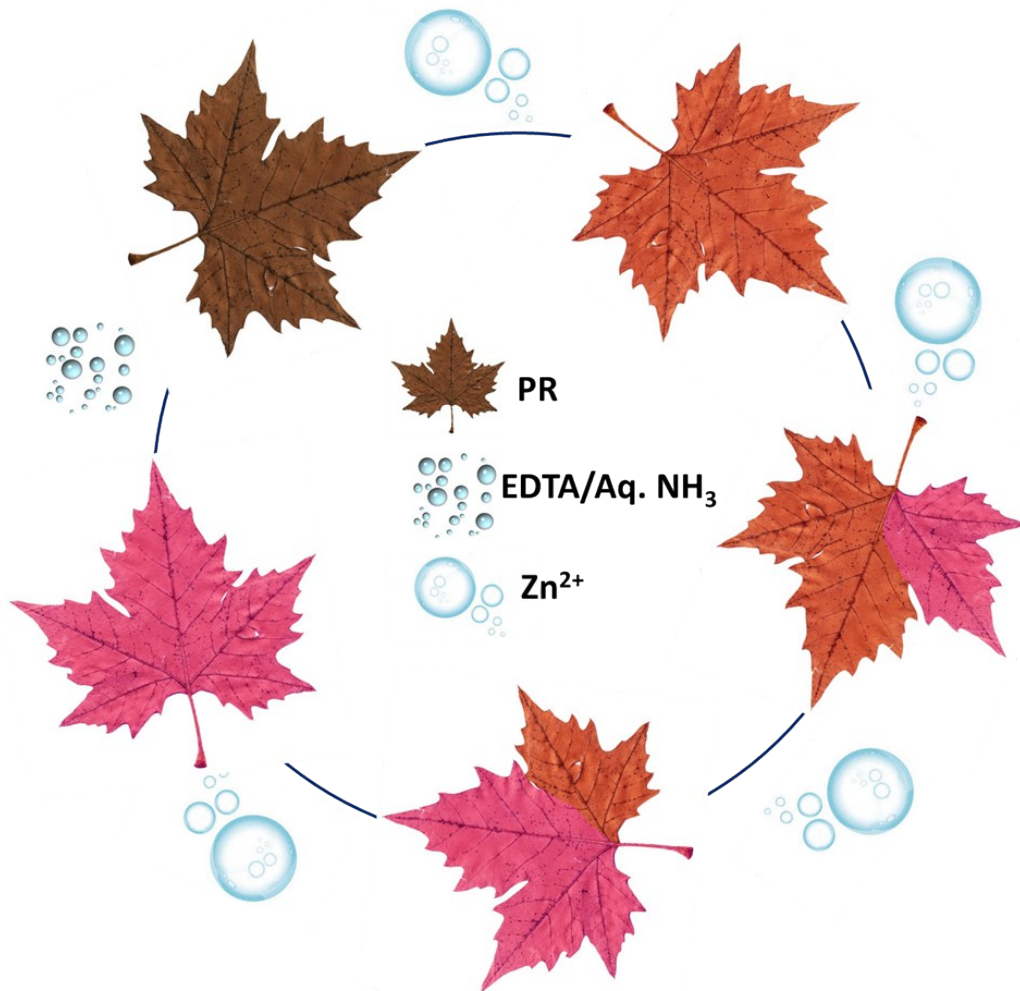


Turn-On fluorescence chemosensor based on a tripodal amine [tris(pyrrolyl- α -methyl)amine]-rhodamine conjugate for the selective detection of zinc ions

Rathinam Balamurugan, Wen-I Chang, Yandison Zhong, Sri Fitriyani and Jui Hsiang Liu*

DOI: 10.1039/b000000x

Graphical picture of PR and response with Zn ²⁺	S2
Determination of quantum yield	S3
Synthesis of RhB1 and H3tpa	S4
Synthesis of H3tpaCO and PR	S5
Fig. S1. ¹ H-NMR spectrum of compound RhB1 in CDCl ₃	S6
Fig. S2. ¹ H-NMR spectrum of compound H3tpa in CDCl ₃	S7
Fig. S3. ¹ H-NMR spectrum of compound H3tpaCO in CDCl ₃	S8
Fig. S4. ¹ H-NMR spectrum of the probe PR in DMSO-d ₆	S9
Fig. S5. . Mass spectrum of the probe PR (a) low resolution (b) high resolution with spectrum	S10
Fig. S6. Effect of pH on fluorescence intensity of PR in CH ₃ CN at 577 nm	S11
Fig. S7. FT-IR spectra of PR (bottom) and PR with Zn ²⁺ (top) S12	
Fig. S8. Time dependent UV-vis spectra (a) and PL spectra (b) of PR with 100 equivalents of Zn ²⁺ in CH ₃ CN/water (9:1 v/v).	S13
Fig. S9. Plots of absorbance (a) and fluorescence intensity (b) time dependence	S14
Fig. S10. Reversible process in UV-vis spectra (a) and PL spectra (b).	S15
Fig. S11. (a) UV-vis spectra of PR in the presence of various zinc salts. (b) PL spectra of PR in the presence of various zinc salts.	S16
Fig. S12. Temperature-dependent ¹ H-NMR spectra of PR with Zn ²⁺ over temperatures ranging from 20 to 80 °C	S17
Fig. S13. Optimized structures of PR and PR-Zn ²⁺	S18
Fig. S14. Hill Plot of fluorescence probe PR with Zn ²⁺ S19	



Graphical picture of PR and response with Zn^{2+}

Determination of fluorescence quantum yield

The quantum yield can be calculated as follows:

$$\Phi_D = \Phi_S \times \frac{F_D}{F_S} \times \frac{A_S}{A_D} \times \frac{(n_D)^2}{(n_S)^2}$$

Where Φ_S is the fluorescence quantum yield of the standard (rhodamine B in ethanol, 0.49, 25°C), F_D and F_S are the integral areas of fluorescence intensity of the chromophore and the standard at the same excitation wavelength, respectively, A_D and A_S are the absorbances of the chromophore and the standard at the defined excitation wavelength, respectively, and n_S and n_D are the refractive indices at 25°C of the solvents of the standard (ethanol) and of the chromophore, respectively.

Synthesis of precursors and the probe

Synthetic routes of precursors and the probe are shown in Scheme 3-1 to 3-3. The following details the experimental conditions and steps.

Synthesis of RhB1

The intermediate **2** was synthesized by refluxing rhodamine B (4.8 g, 10 mmol) with excess ethylenediamine (5 mL) in ethanol until the solution lost its red color. After completion of the reaction, the solvent was removed by rotary evaporator. The resultant solid was extracted with dichloromethane and washed with water several times. The organic layer was separated and dried over anhydrous MgSO₄, and then the solvent was removed thoroughly. The resultant solid was washed with hot hexane (10 mL) and dried. Finally, the crude solid was purified by column chromatography (eluent, EA: Hexane = 1:3, R_f = 0.45) ^{13a,b}.

Yield= 80%. ¹H-NMR (400 MHz, CDCl₃) δ: 7.88–7.90 (d, 1H, ArH), 7.42–7.45 (m, 2H, ArH), 7.07–7.09 (d, 1H, ArH), 6.26–6.43 (m, 6H, ArH), 3.20–3.35 (q, 8H, NCH₂CH₃), 3.17–3.18 (t, 2H, NCH₂CH₂N), 2.41–2.43 (t, 2H, NCH₂CH₂N), 0.85–1.55 (t, 12H, NCH₂CH₃).

Molecular formula: C₃₀H₃₂N₄O₂ (484 g/mol).

Synthesis of Tris(pyrrolyl- α -methyl)amine (H₃tpa) (**3**)

Compound **3** was synthesized by following reported procedures¹⁴. Pyrrole (18 g), 37% aqueous formaldehyde (20 mL), NH₄Cl (4.78 g), ethanol (60 mL) and water (20 mL) were mixed in a 250 mL flask. The mixture was stirred at 40°C for 1 h. Then, it was poured into 200 mL of water and extracted three times with ethyl acetate. The combined organic phase was dried over anhydrous MgSO₄. After reaction, the solvent was removed by rotary evaporation. Remaining pyrrole impurities were removed by extracting the crude mixture in a mixture of ether (30 mL), THF (30 mL), and 20% NaOH_(aq). The upper layer of the mixture was collected and concentrated. After evaporation, pure compound **3** was observed.

Yield= 77%. ¹H-NMR (400 MHz, CDCl₃) δ: 8.2 (s, 3H, NH), 6.7 (s, 3H, ArH), 6.12–6.16 (t, 3H, ArH), 6.07 (s, 3H, ArH), 3.58 (s, 6H, NCH₂).

Molecular formula: C₁₅H₁₈N₄ (254 g/mol).

Synthesis of Tris(5-formylpyrrol-2-ylmethyl)amine (H_3tpa^{CO}) (**4**)

The intermediate **4** was acquired from the Vilsmeier–Haack formylation of **3**. The intermediate **3** (2 g) was dissolved in dimethylformamide (40 mL) and cooled to -10°C . POCl_3 (4.4 mL) was added dropwise over 10 minutes with vigorous stirring, and the solution became dark red. The mixture was removed from the ice bath and heated to 60°C for 2 h. An aqueous NaOH solution (6.00 g) were prepared and poured into the mixture. Then, the mixture was heated to 80°C for 1 h. After the reaction, it was cooled to room temperature and extracted with DCM:chloroform (1:1). The solvent was removed by rotary evaporator, yielding an oily crude product. This oily crude product was stirred with a large excess of acetonitrile for 16 h to precipitate the product **4**. The precipitate was filtered, washed with acetonitrile and dried. Product **4** was obtained as pale brown solid¹⁵.

Yield= 73%. $^1\text{H-NMR}$ (400 MHz, CDCl_3) δ : 11.19 (s, 3H, CHO), 9.39 (s, 3H, NH), 6.91–6.92 (d, 3H, ArH), 6.17–6.18 (d, 3H, ArH), 3.69 (s, 6H, NCH_2).

FTIR (KBr, $\nu_{\text{max}}/\text{cm}^{-1}$): 3457 (NH), 2766 (CHO), 1612 (CO).

Molecular formula: $\text{C}_{18}\text{H}_{18}\text{N}_4\text{O}_3$ (338.36 g/mol).

Synthesis of Pyrrol-Rhodamine Chemosensor (**PR**)

A solution of ethylenediaminyl Rhodamine B (1.18 g, 0.74 mmol) in anhydrous ethanol (50 mL) was added to the intermediate **4** (0.25 g, 2.44 mmol) and stirred for 2 days at 80°C . After completion of the reaction, the solvent was removed by rotary evaporation. The crude product was further purified and isolated by column chromatography (silica gel, 100–200 mesh) using methanol in DCM (10% v/v) as eluent.

Yield= 70%. $^1\text{H-NMR}$ (400 MHz, DMSO) δ : 10.98–11.95 (s, 3H, NH), 7.72–7.90 (s, 3H, CHN), 7.41–7.71 (m, 9H, ArH), 6.99–7.10 (d, 3H, ArH), 6.24–6.39 (m, 21H, ArH), 5.92–5.97 (d, 3H, ArH), 3.12–3.50 (m, 42H, NCH_2), 1.01–1.10 (t, 36H, CH_2CH_3). $^{13}\text{C-NMR}$ (400 MHz, CDCl_3) δ : 168 (CO), 154 (CHN), 149 (Ar), 134 (ArH), 132 (Ar), 129 (ArH), 128 (ArH), 127 (ArH), 124 (ArH), 122 (ArH), 118 (ArH), 118 (ArH), 116 (Ar), 98 (ArH), 78 (Ar), 77 (Ar), 65 (NC-Ar), 50 (NCH_2), 44 (NCH_2CH_3), 42 (CHN-CH_2), 41 (NCH_2), 17 (CH_2CH_3).

Mass spectrum (FAB, m/z): 1739 (M), Molecular formula: $\text{C}_{108}\text{H}_{120}\text{N}_{16}\text{O}_6$ (1738 g/mol).

RhB-NH2 CDCl3 2014/12/11 AV500

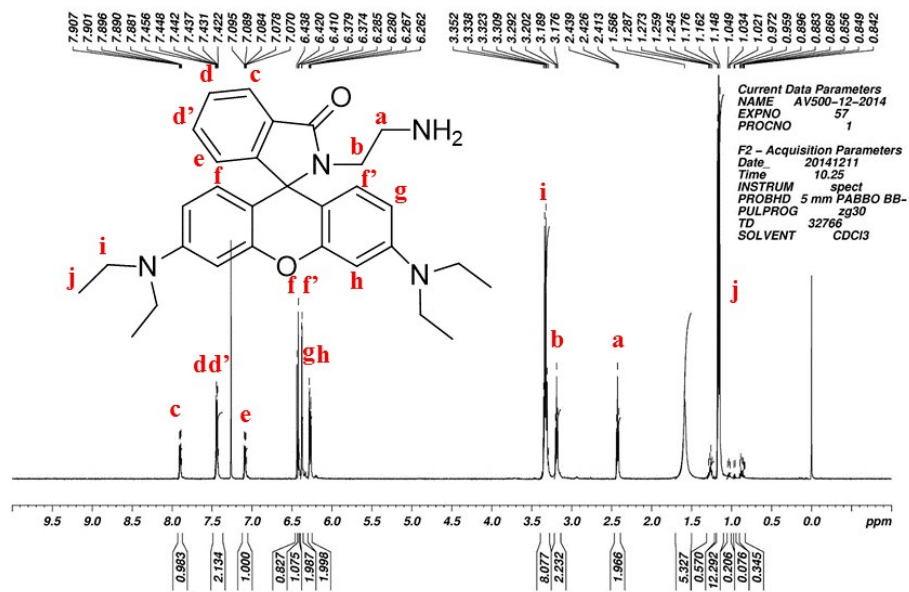


Fig. S1 ¹H-NMR spectrum of compound RhB1 in CDCl₃

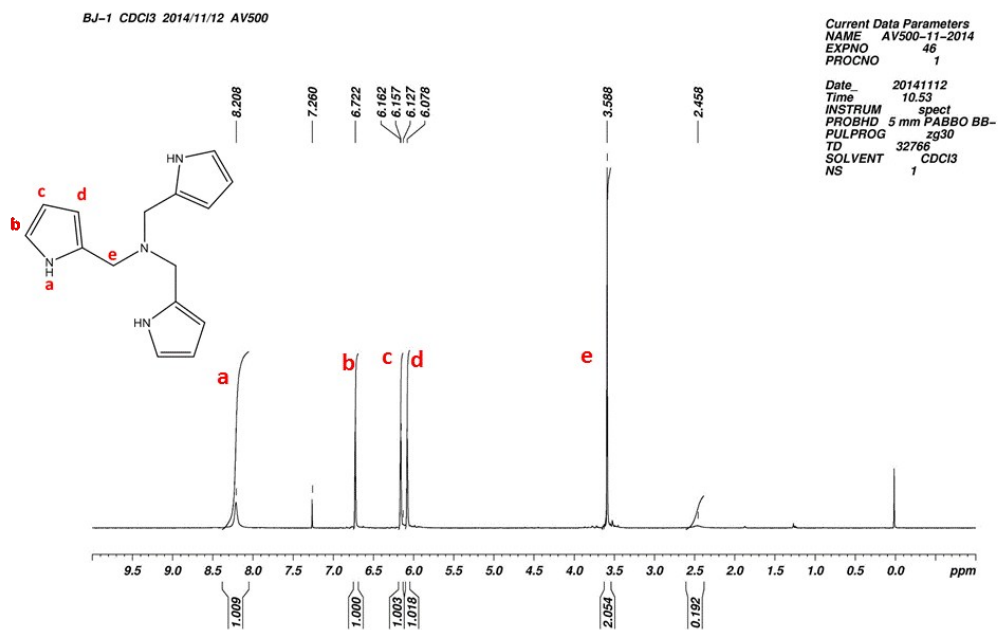


Fig. S2. ¹H-NMR spectrum of compound H₃tpa in CDCl₃.

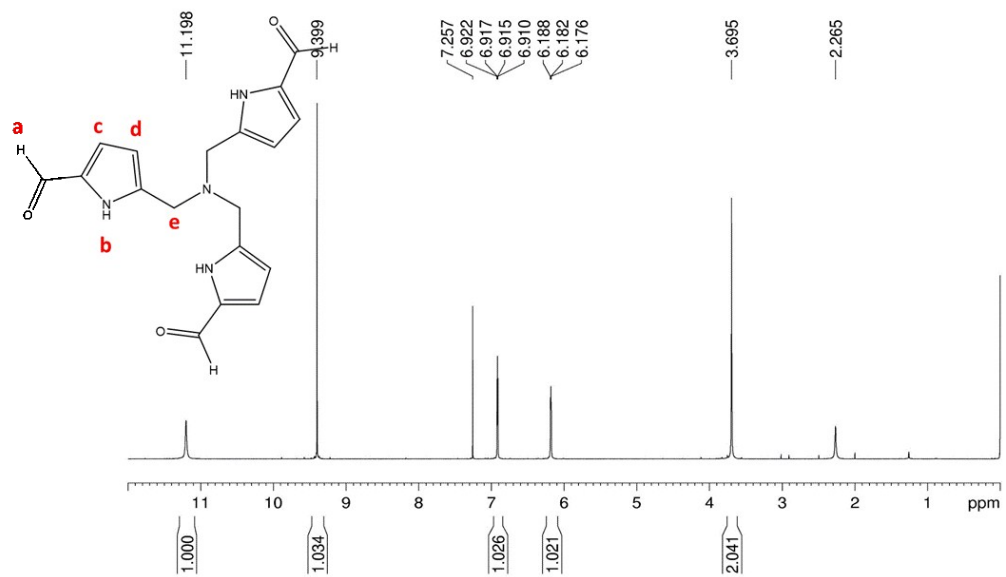


Fig. S3. 1H -NMR spectrum of compound H_3tpa^{CO} in $CDCl_3$.

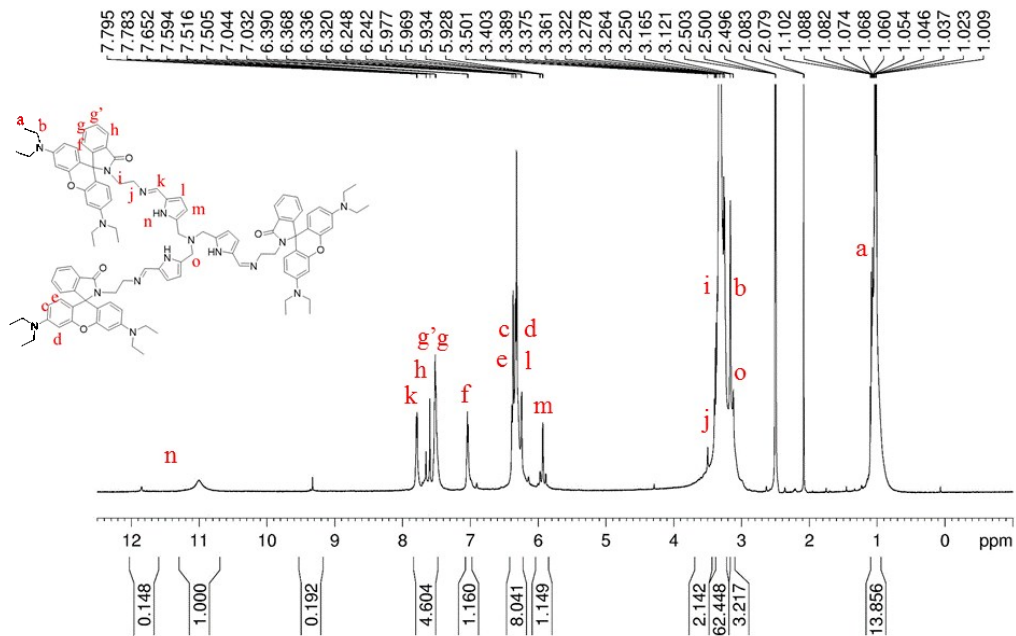


Fig. S4. ¹H-NMR spectrum of probe the PR in DMSO-d₆.

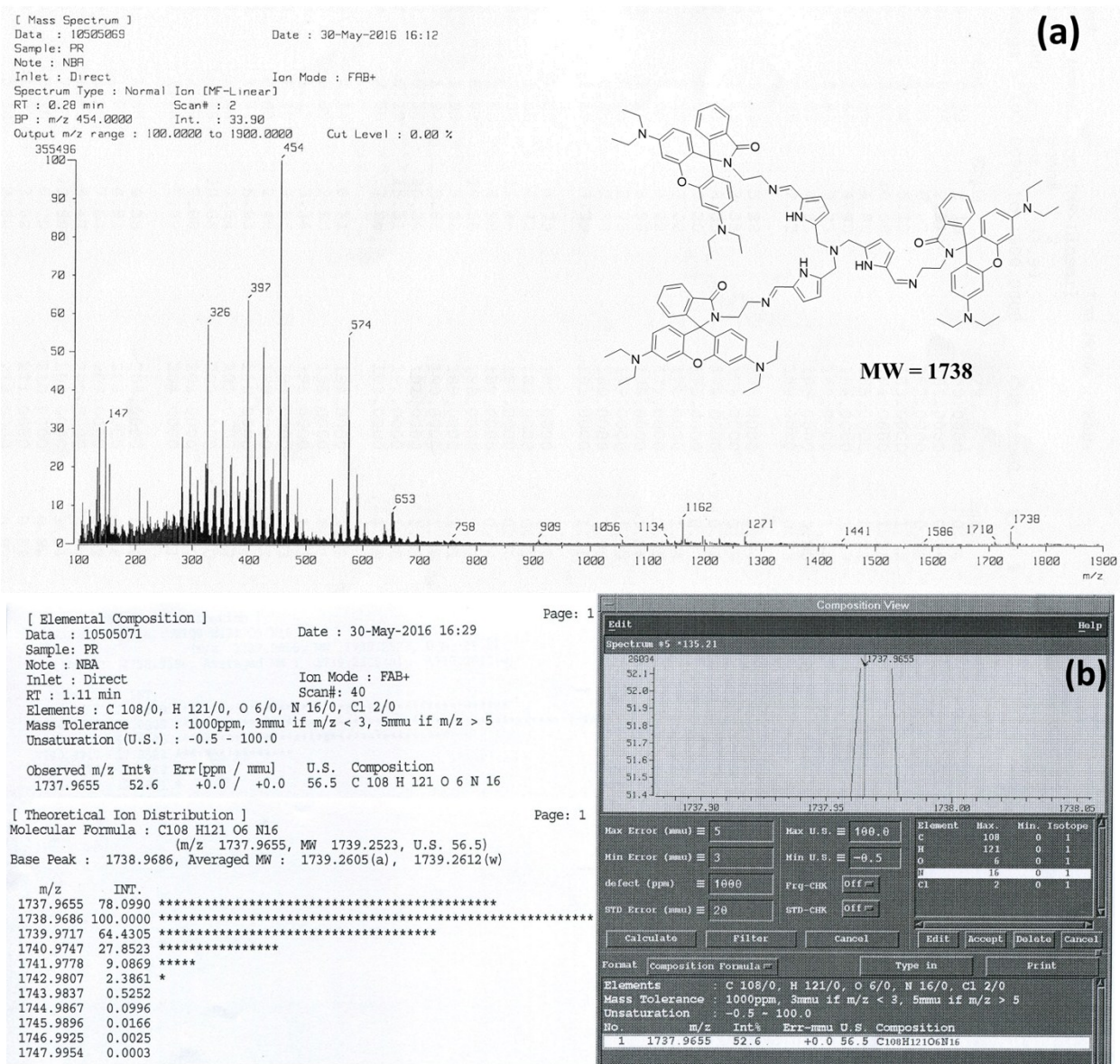


Fig. S5. Mass spectrum of the probe **PR** (a) low resolution (b) high resolution mass spectral data with spectrum

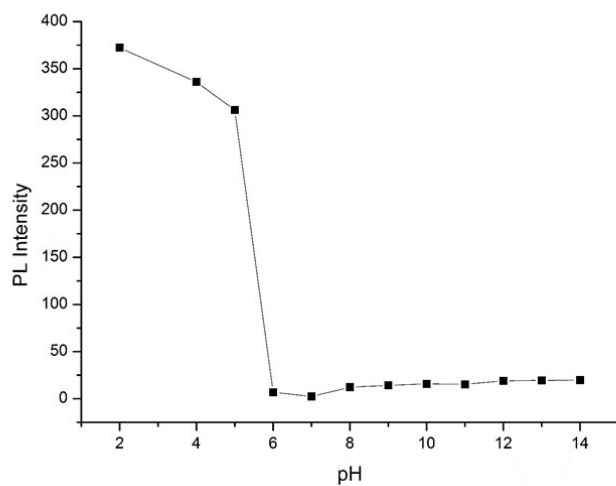
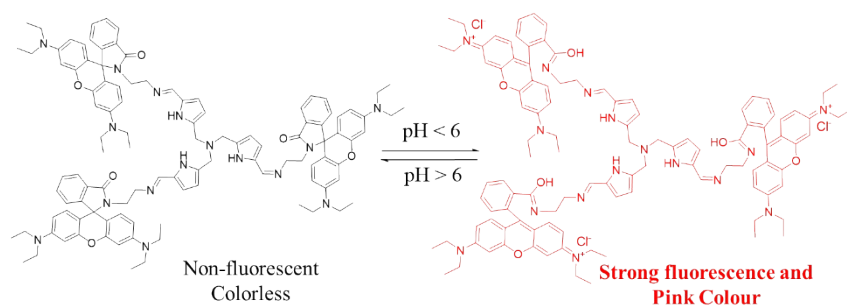


Fig. S6. Effect of pH on fluorescence intensity of **PR** in $\text{CH}_3\text{CN}:\text{H}_2\text{O}$ (1:1 v/v) at 577 nm. The pH of the solutions was adjusted by HCl (1 M) and NaOH (1 M), $\lambda_{\text{ex}} = 520 \text{ nm}$

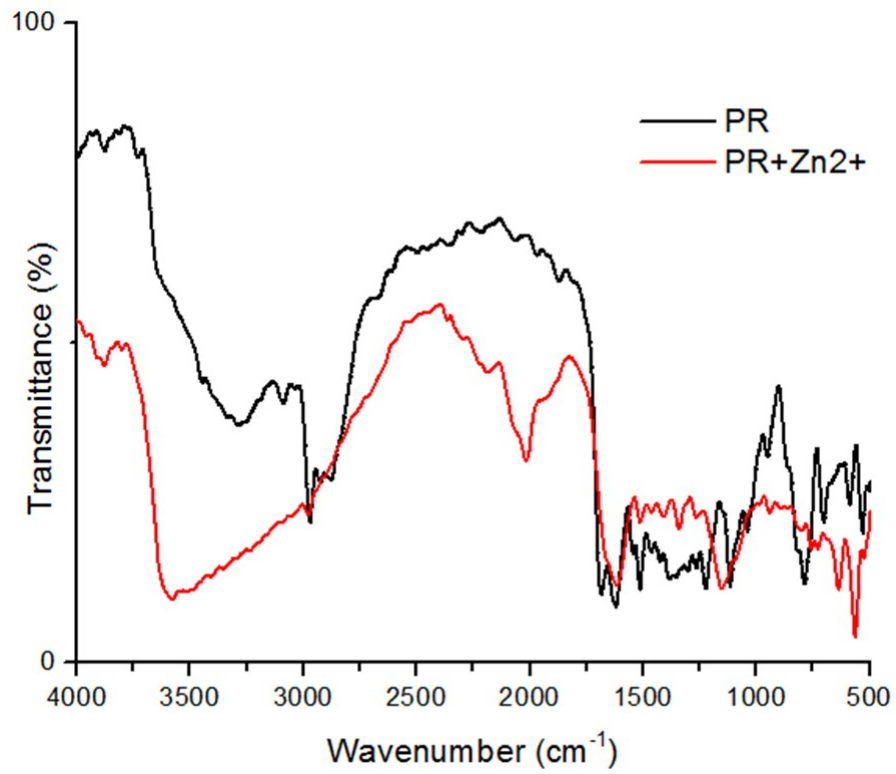


Fig. S7. FT-IR spectra of **PR** and PR-Zn²⁺ complex

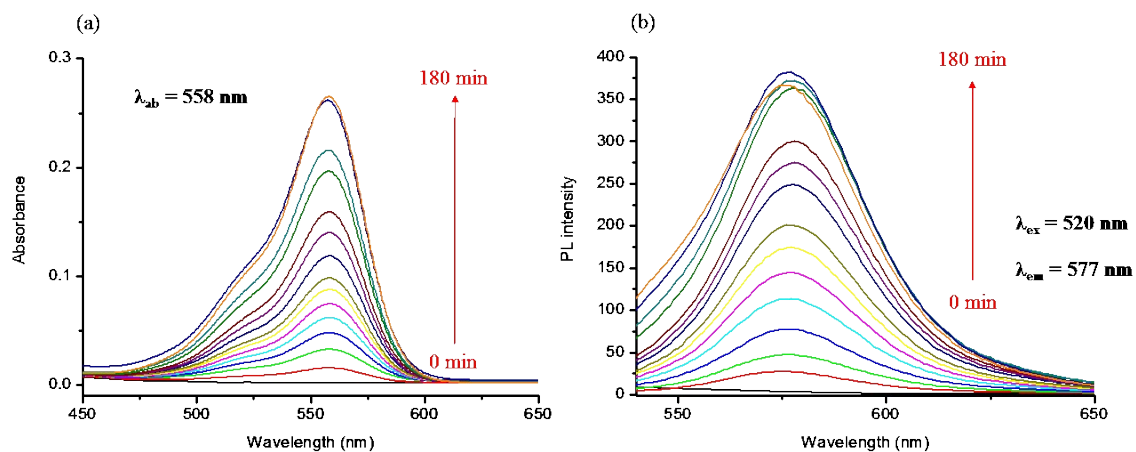


Fig. S8. Time dependent UV-vis spectra (a) and PL spectra (b) of PR with 100 equivalents of Zn²⁺ in CH₃CN/water (1:1 v/v).

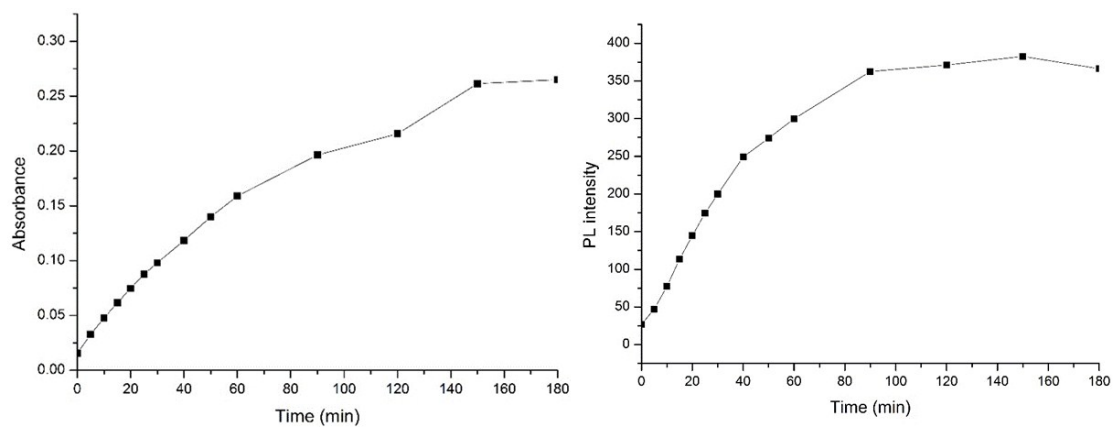


Fig. S9. Plots of absorbance (a) and fluorescence intensity (b) time dependence

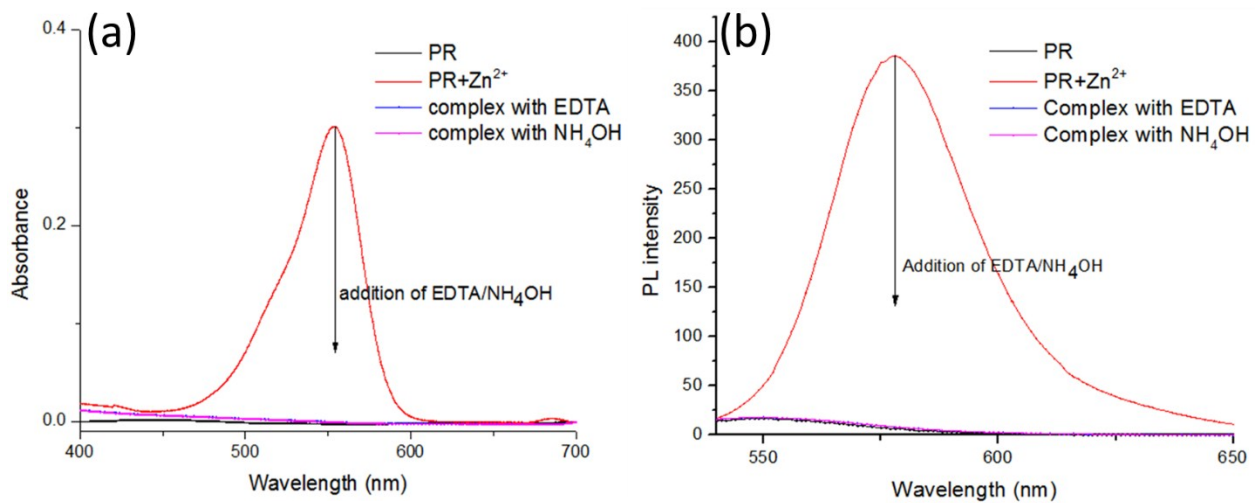


Fig. S10. Reversible process in UV-vis spectra (a) and PL spectra (b).

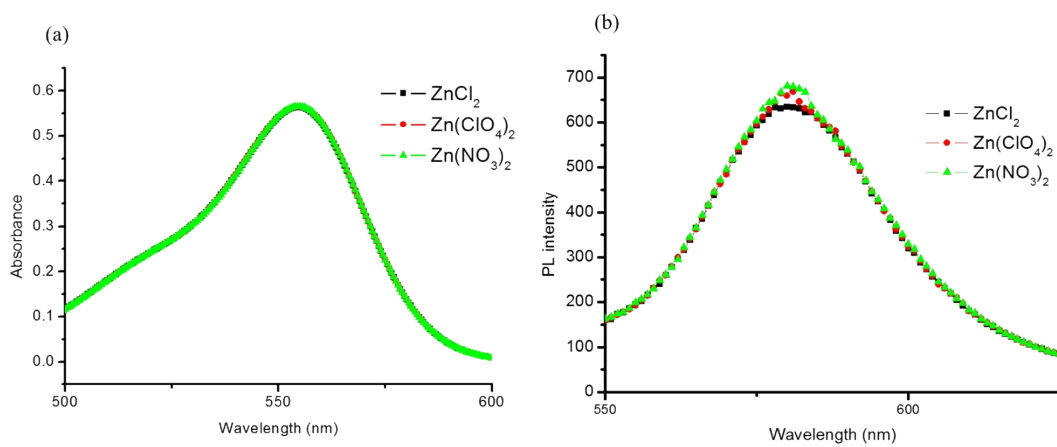


Fig. S11. (a) UV-vis spectra of **PR** in the presence of various zinc salts.

(b) PL spectra of **PR** in the presence of various zinc salts.

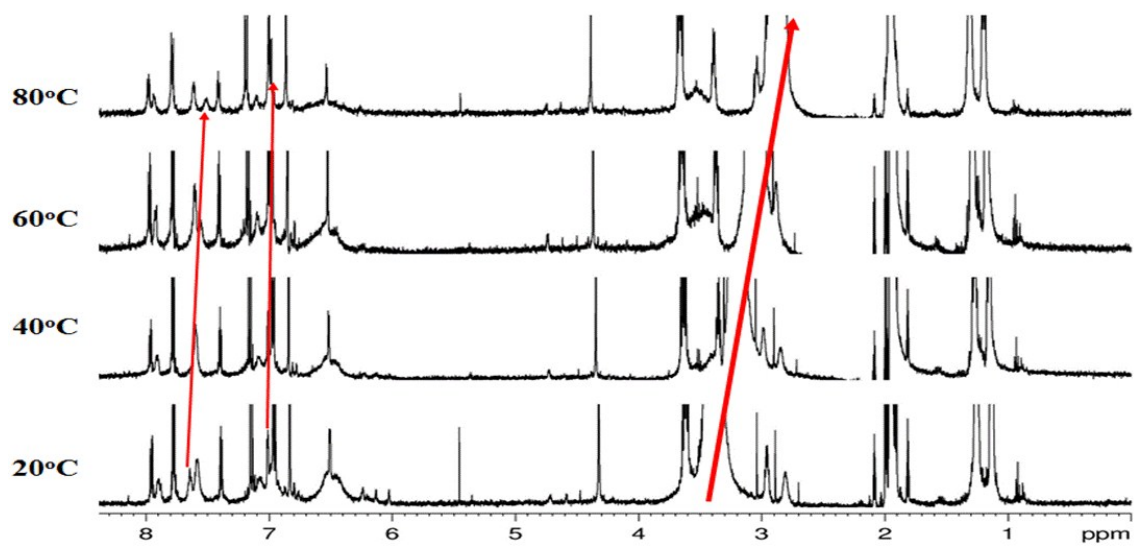


Fig. S12. Temperature dependent ¹H-NMR spectra of **PR** with Zn²⁺ over temperatures ranging from 20 to 80°C

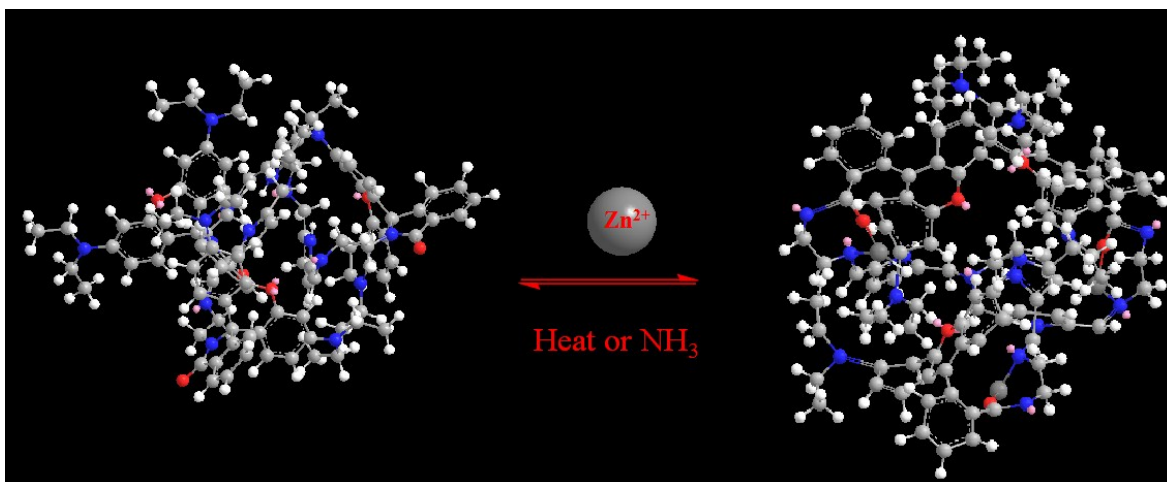


Fig. S13. Optimized structures of PR and PR-Zn²⁺.

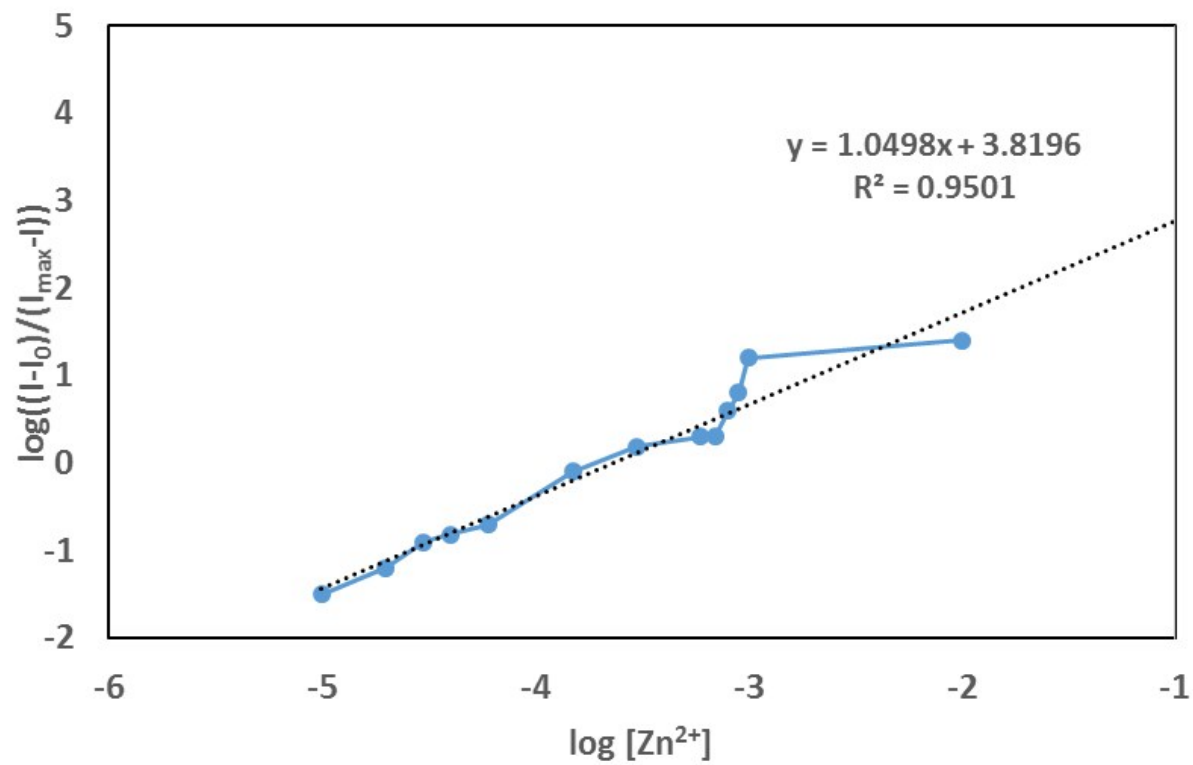


Fig. S14 Hill Plot of fluorescence probe PR with Zn^{2+}